

# Chapter 17

## Design of Valve Train for Heavy Duty Application



Aniket Basu, Nitin Gokhale, Yogesh Aghav and M. N. Kumar

**Abstract** Today's high speed and heavy-duty engine demands precise design and analysis of the various engine components. Amongst the various components, valve train of an Internal Combustion (IC) engine plays the crucial role. The components of valve train like camshaft, tappet, pushrod, rocker arm, valves etc. are subjected to inertia and vibrational forces. The valves are also subjected to thermal loads. These forces should be studied to make sure precise and controlled functioning of the valve train. The complex task of valve train system design and development can be achieved by theoretical and simulation analysis which considers mechanical, thermal and hydrodynamic factors. Different simulation tools are available for valve train kinematic analysis. This chapter describes about the methods of cam design, valve train layouts, theoretical analysis of valve train design and comparison with simulation results, tribology of valve train and experimentation of valve train.

### 17.1 Valve Train

A schematic sketch of a typical valve train is shown in Fig. 17.1. In an overhead valve or pushrod engine the camshaft is in the cylinder block and valves are in the cylinder head. Figure 17.2a shows various types of valve trains and their typical characteristics along with a flowchart for valve train system design in Fig. 17.2b (Wang 2006).

Type 1 valve train is the direct acting OHC (Overhead cam) design. This valve train has the highest stiffness amongst all valve train designs and is suitable for high speed applications. The height of the engine is generally large and roller tappets cannot be used resulting in higher friction. Valve lash adjustment is also critical for this type of design.

Type 2 valve train is also known as finger follower design; it is an OHC type of design with end pivot rocker arm. In roller configuration this valve train gives low

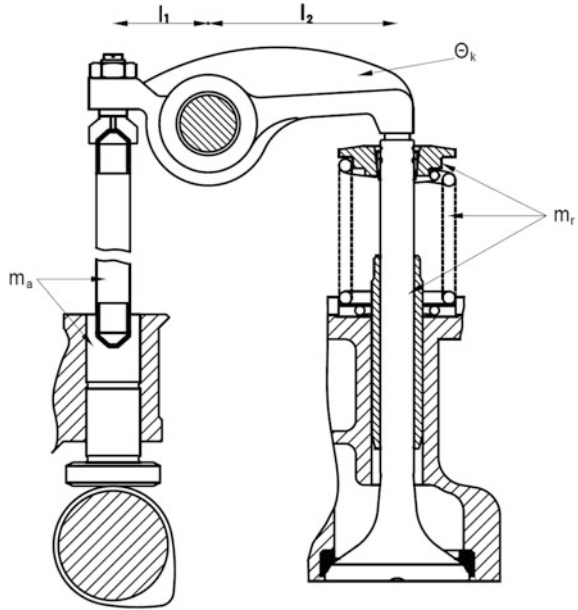
---

A. Basu · N. Gokhale (✉) · Y. Aghav · M. N. Kumar  
Kirloskar Oil Engines Ltd., Pune, India  
e-mail: [Nitin.Gokhale@kirloskar.com](mailto:Nitin.Gokhale@kirloskar.com)

© Springer Nature Singapore Pte Ltd. 2020  
P. A. Lakshminarayanan and A. K. Agarwal (eds.), *Design and Development of Heavy Duty Diesel Engines*, Energy, Environment, and Sustainability,  
[https://doi.org/10.1007/978-981-15-0970-4\\_17](https://doi.org/10.1007/978-981-15-0970-4_17)

601

**Fig. 17.1** Typical overhead valve train



friction and high rocker ratios are possible. Hydraulic lash adjuster can be easily integrated. This design has lower stiffness compared to type 1.




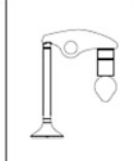
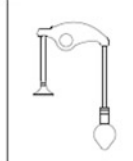
Type 3 design is also an OHC design but with centre pivot rocker arm. The Type 3 valve train has low friction in the roller follower mode and low engine height. It has relatively simple design with high stiffness and can be used for high speed applications. Furthermore, it is difficult to incorporate the hydraulic adjustment, and its friction can be high if a shaft is used as the pivot without a rolling element.

Type 4 valve train is an OHC valve train with a centre-pivot rocker and cam follower directly acting on the rocker arm without a pushrod. The cam follower can be a flat face or roller hydraulic lifter. It has the highest weight and number of components amongst all OHC designs.

Type 5 design has an overhead valve design with cam being placed in the block. Camshaft is directly gear driven from crank. This design is simplest to adopt and one of the most widely used designs. It has low stiffness, low cost, and it is easy to adapt to hydraulic lash compensation and roller followers. Most of the discussion in this chapter will focus on design and development of Type 5 valve train.

Figure 17.2b also shows the typical flowchart of valve train system design which requires considerations from geometrical design and packaging, kinematics, flow through valves and dynamics. Depending on application some aspects may have higher priority over other resulting into various design decisions regarding valve train.

(a)

					
	Type I	Type II	Type III	Type IV	Type V
Natural Frequency(Hz)	2000 - 3000	1200 - 1600	900 - 1400	900 - 1400	400 - 700
Effective Mass Valve(g)	140 - 160	80 - 120	120 - 160	130 - 170	240 - 290
Maximum Speed (rpm)	6500++	6500++	6000++	6000++	4000 - 6000
Friction	E	A	B	C - D	C - D
Overall Engine Packaging	D - E	D - E	B	C	A

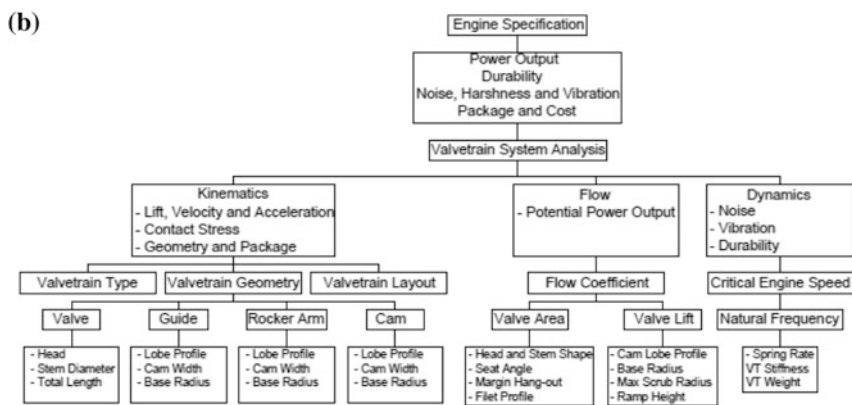


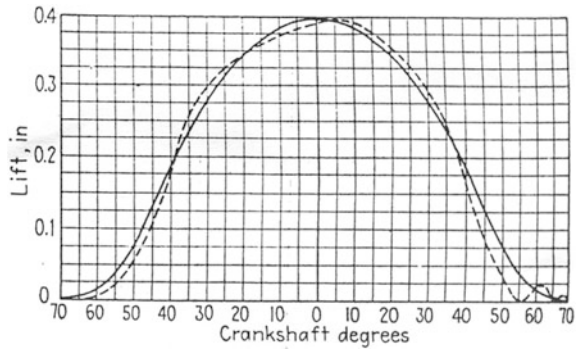
Fig. 17.2 a Different valve train design concepts and valve train design flowchart b Valve train system design flowchart

## 17.2 Valve Train Design

In valve train system design first starts by defining the valve opening and closing events for the target volumetric efficiency. Once the timing of valve events has been established the shape of the cam can be determined. Before going into design of actual cam profile various other design decisions have to be made with respect to the layout of the valve train. Following are some of the steps followed for the complete valve train layout.

**Valve sizing:** In this step the basic sizing of the valve inner seat diameter, head diameter and stem diameter is done. Stem diameter is generally 1/5 to 1/6 of head diameter for a stable design. This is generally based on flow requirements and is generally done along with detailed layout of valve and seat. Valve positions are also finalized at this stage. A small angular difference is kept between valve and seat for effective sealing.

**Fig. 17.3** Theoretical and actual valve lift curves



**Valve Guide and Spring layout:** This step will decide the height of the valves and the cylinder head. It is generally recommended that 40% of the valve length is supported in guide and 60% of guide is supported in the cylinder head. Initial spring layout is carried out considering the required spring preload and stiffness requirements. A good starting point for spring OD is generally between 30–40% of cylinder bore diameter for a 2-valve configuration.

**Lever Layout:** Next step is to finalize the positions of the levers, lever support and oil supply arrangement for lever bushes, lash adjuster if any. Rocker ratios and pushrod positions in the cylinder head are also done simultaneously at this stage.

**Camshaft layout, cam design:** In this step the cam shaft position in the block, cam width, tappet diameter and journal diameter are decided. In cam design the first step is to fix the size of the cam base circle. This is normally made as large as possible within the limits imposed by the cam shaft bearing journal diameter. Lift must be corrected by the rocker arm ratio in the event that an overhead valve gear is under consideration. In order to avoid excessive jerk, the corners of the acceleration curve particularly an opening and closing are generously rounded. In order to achieve the desired goal of smooth motion with low shock loading the transition between the base circle and flank of the cam must be carefully designed. A ramp is used on the opening and closing sides of the cam. This provides margin that can accommodate length changes in the valve train that results from wear or thermal effects where solid tappets are used or that can accommodate leak down in the instances where hydraulic tappets are used. Due to elasticity of parts the actual and theoretical valve lift curves vary. This is shown in following Fig. 17.3.

## 17.3 Calculation of Cam Profile

### 17.3.1 Harmonic Cam

Harmonic cams are used for high speed engines are formed to shape in compliance with a pre-selected manner of valve motion. A smooth and continuous change in the



**Table 17.1** Cam design formulae

Section	Section description	Lift, $h_0$	$h_{end}$	Velocity, $\omega_f$	Acceleration, $J_f$
		mm	(e.g., $h_{1c}$ etc.)	mm/cam deg	mm/cam deg <sup>2</sup>
0	Ramp	$\Delta s (1 - \cos (\pi / 2\Phi_0) \varphi_{C0})$	–	$\Delta s \omega_c \pi / 2\Phi_0 \sin (\pi / 2\Phi_0) \varphi_{C0}$	$\Delta s \omega_c^2 (\pi / 2\Phi_0)^2 \cos (\pi / 2\Phi_0) \varphi_{C0}$
1	Acceleration	$\Delta s + c_{11} \varphi_{C1} - c_{12} \sin (\pi / \Phi_1) \varphi_{C1}$	–	$\omega_c [c_{11} - c_{12} (\pi / \Phi_1) \cos (\pi / \Phi_1) \varphi_{C1}]$	$\omega_c^2 [c_{12} (\pi / \Phi_1)^2 \sin (\pi / \Phi_1) \varphi_{C1}]$
2	Initial deceleration	$h_{1c} + c_{21} \varphi_{C2} + c_{22} \sin (\pi / 2\Phi_2) \varphi_{C2}$	$\Delta s + c_{11} \Phi_1$	$\omega_c [c_{21} - c_{22} (\pi / 2\Phi_2) \cos (\pi / 2\Phi_2) \varphi_{C2}]$	$\omega_c^2 [-c_{22} (\pi / 2\Phi_2)^2 \sin (\pi / 2\Phi_2) \varphi_{C2}]$
3	Final deceleration	$h_{2c} + c_{31} (\Phi_3 - \varphi_{C3})^4 - c_{32} (\Phi_3 - \varphi_{C3})^2 + c_{33}$	$\Delta s + c_{11} \Phi_1 + c_{21} \Phi_2 + c_{22}$	$\omega_c [-4 (\Phi_3 - \varphi_{C3})^3 + 2 c_{32} (\Phi_3 - \varphi_{C3})]$	$\omega_c [12 (\Phi_3 - \varphi_{C3})^2 - 2 c_{32}]$

1. tapering,  $\phi_0$ , a cosine curve
2. positive acceleration,  $\phi_1$ , half the sine wave
3. first section of negative acceleration,  $\phi_2$ ,  $1/4$  sine wave
4. second section of negative acceleration,  $\phi_3$ , a segment of parabola

Figure 17.5 shows the polar representation of the same.

Above table contains formulae to calculate lift velocity and acceleration.

**Pressure Angle**

The pressure angle of a cam is the angle between the line of motion of the follower and the normal to the cam surface at the point of contact between the cam and follower.

$$\alpha = \frac{1}{R} \frac{dr}{d\theta}$$

where  $\alpha$  is pressure angle (1.1)

**Radius of Curvature**

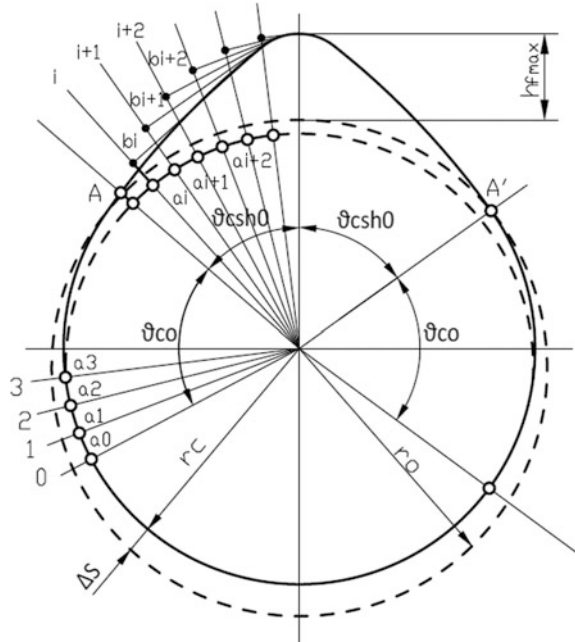
It is a measure of the rapidity with which the curve changes the direction.

$$\rho = \frac{d^2h}{d\theta^2} + h + R_B \tag{17.2}$$

where

- $\rho$  radius of curvature, mm,
- $\theta$  cam angle in radian and
- $R_B$  base circle radius, mm

Fig. 17.5 Cam shape



**Polydyne Cam**

Another very popular method of designing the cam profile is the Polydyne cam method. It is the standard cam form for high speed engines. This uses a polynomial to calculate the valve lift curve in the main event of the cam contour. This cam form makes allowance for the static and dynamic deflections of the valve train at the design speed of the cam. The design of polydyne cam is carried out in three principal steps. In the first step, the valve lift curve is defined by the higher order polynomial. In a second step, the equivalent tappet lift referred to the valve is determined under the consideration of the deflections of the valve train at cam design speed. In a third step the actual cam profile is determined under consideration of the actual valve train geometry. This step also includes the evaluation of cam profile radii, of cam tappet contact stresses etc.

The following polynomial is used for the evaluation of the valve lift curve.

$$y = L(1 + C_2X^2 + C_4X^4 + C_pX^p + C_qX^q + C_2X^2 + C_rX^r + C_5X^5) \tag{17.3}$$

Here, L = maximum lift above ramps at  $x = 0$ .

- Y lift at any point  $0 \leq x \leq 1$ .
- $C_2, C_4, C_p, C_s$  coefficients.

$X$   $\theta/a$  where  $\theta$  = cam angle counted from the point with maximum lift  
 $a$  half main event length and p, q, r, s are exponents

The above coefficients are described from the boundary conditions.

$C_4$  is a freely chosen coefficient by which the shape of the negative acceleration curve could be varied for an optimizing of the cam profile.

The polydyne cam design method here is based on an equivalent two mass system of valve train as shown in the Fig. 17.6. Two masses connected by a spring represent the valve train stiffness and the contact with this spring is maintained by the pre-loaded valve spring.

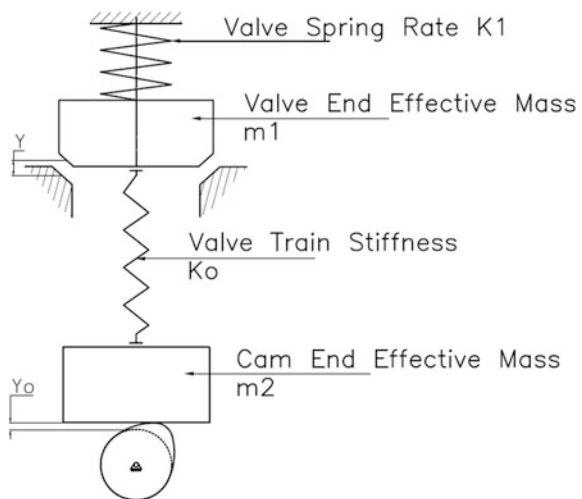
**Constant Velocity Ramp Type**

The constant velocity ramp has generally been used as a standard ramp for high speed I.C. engines with mechanical valve lash adjustment. This ramp type consists of a constant velocity section adjacent to the main event and a constant acceleration section at the end of the ramp at the transition to the base circle. In general, the length of constant velocity section is determined from the condition that the lift at the end of this section is  $1/4$  of the total ramp height. A typical ramp provided on the cam profile is as shown in Fig. 17.7. Some of the other types of ramps used in cam profile design are cosine ramp and trapezoidal acceleration ramp.

**Radii of the Cam Contour**

For cams operating on a flat faced follower the radii of the cam contour are obtained from the following relation. Figure 17.8 shows the typical nature of cam contour radius for flat follower. The minimum value occurs at nose and should not be less than 3 mm to avoid very high contact stresses.

Fig. 17.6 Two mass system





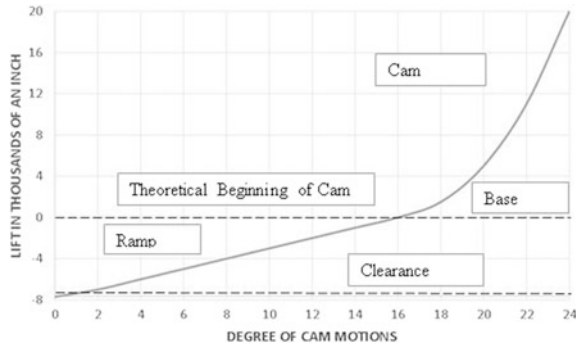


Fig. 17.7 Representation of ramp on the cam profile

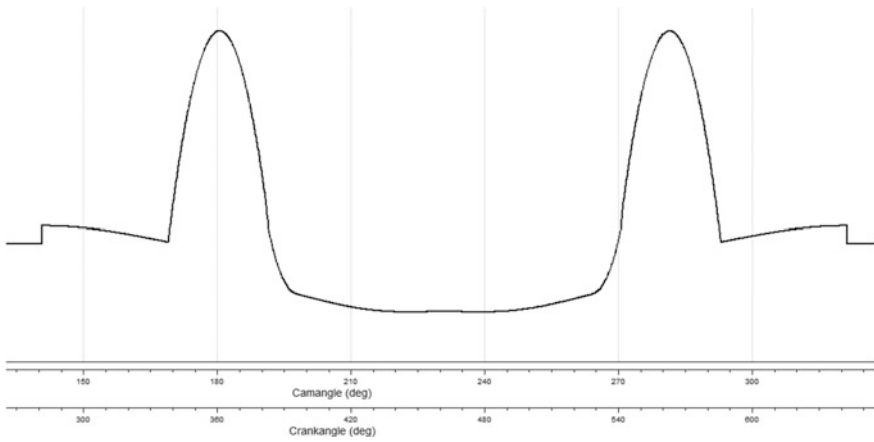


Fig. 17.8 Radius of cam contour

$$R = R_B + Z_0 + Z_0'' \left( \frac{180}{\pi} \right)^2 \tag{17.4}$$

where,

$R_B$  base circle radius, mm

$Z_0$  tappet lift, mm.

$Z_0''$  second derivation of the tappet lift with respect to the cam angle

## 17.4 Parameters for Evaluation of the Cam Design

### 17.4.1 Required Length of the Positive Acceleration Pulse

The polydyne method results in a theoretically complete compensation of valve train vibrations at design speed. Below design speed a maximum of vibration occurs at 70% of the design speed. Equal vibration amplitudes as at 70% of design speed also occur at 110% of the design speed. Above these 110% of the design speed the vibration amplitudes rise indefinitely. Operation at higher than 110% of the design speed should be excluded therefore by a proper choice of the design speed.

To obtain a low vibration operation of the valve train at all speeds of the design speed the length of the positive acceleration pulse should be at least 1.2–1.3 times the angle of camshaft rotation occurring within the time of one valve train vibration at design speed.

$$\Theta_r = (1.2 - 1.3) \frac{360N_c}{f_N} \quad (17.5)$$

Here,

$\Theta_r$  required length of the positive acceleration pulse of the equivalent tappet acceleration  $y''$

$N_c$  camshaft design speed, rpm

$f_N$  valve train natural frequency, cycles/min

A further condition which has to be observed in the choice of the length of the positive acceleration pulse is the avoidance of hollow flanked cam profiles or unacceptable small concave flanked radii as a consequence of too high cam accelerations, if a curved follower is used.

Required valve spring force.

In dynamic respect the valve spring force must be to keep the valve train components in contact over the entire engine speed range including an allowance for friction and valve train vibrations.

$$\left( \frac{F_s}{F_d} \right)_{\min} \geq 1.1 - 1.2 \quad (17.6)$$

As per the experience with high speed engines this condition is met as far as valve spring forces exceed the theoretical deceleration force at maximum engine speed by at least 10–20% over the whole deceleration period. The theoretical deceleration force at maximum engine over speed is obtained from the relation

$$F_d = 36N_{\max}^2 (m_1 y_0'' + m_2 z_0''/i) \quad (17.7)$$

(Its values are given at corresponding cam angle degrees in the form of graph.)

Here,

- $N_{max}$  camshaft rpm at maximum engine speed  
 $m_1, m_2$  valve end and cam end mass respectively  
 $I$  instantaneous rocker ratio

Cam to tappet contact stress

In the instance of a flat faced follower the cam to tappet contact stress (Hertz-stress) becomes

$$S_c = 0.418 \sqrt{\frac{FE_m}{WR}} \quad (17.8)$$

(Its values are given at corresponding cam angle degrees in the form of graph.)

Here,

$F$  = force acting between cam and tappet,

$E_m = \frac{2E_1E_2}{E_1 + E_2}$ , mean modulus of elasticity between cam and tappet material.

$W$  contact width between cam and tappet.

$R$  radius of the cam contour in the point of contact.

The higher contact forces certainly occur in the acceleration period at high speed operation where spring and inertia forces are superimposed. In this cam section, however, the radii of the cam contour are so big that the contact stresses do not normally reach a critical level. The more contact stresses with a flat faced tappet therefore normally occurs in the nose section the cam where the radii of the cam contour are normally small. In this section the inertia forces counteract the spring forces. The maximum contact loads therefore occur at the low speed operation where the inertia forces are small and the cam tappet contact is loaded with almost the full spring force times the rocker arm ratio. The evaluation of the contact stresses in the cam nose section therefore is based on the extreme assumption of negligible small inertia forces which assumption yields an upper limit for the actual maximum contact stresses.

## 17.5 Hydrodynamic Evaluation Coefficient for Lubricating Conditions Between Cam and Tappet

The consideration of the effective hydrodynamic velocity between cam and tappet in Dowson's and Higginson's formulas for the minimum oil film thickness yields the following relation for the minimum oil film thickness between cam and tappet.

$$h_{min} = K(R_B + Z_0) \sqrt{2 \left( \frac{R}{R_B + Z_0} \right)^2 - \left( \frac{R}{R_B + Z_0} \right)} \quad (17.9)$$

The coefficient  $k$  includes the camshaft speed and the oil viscosity and need not be considered for comparison of the cam profiles for a particular engine. In such a comparison only the ratio,

$$\gamma = \frac{R}{R_B + Z_0} \quad (17.10)$$

is decisive for the magnitude of the minimum oil film thickness. This criterion therefore is designated the hydrodynamic evaluation coefficient.

- $R$  radius of the cam contour at the contact point.  
 $R_B$  base circle radius.  
 $Z_0$  tappet lift

According to the above relation the minimum oil film thickness is zero for  $\gamma = 0$  and  $\gamma = 0.5$ . Between these two values an optimum oil film thickness is achieved with  $\gamma = 0.25$ . Furthermore, a rapid increase of oil film thickness occurs in the range  $\gamma > 0.5$ . In general the geometric conditions on the cam nose yield HEC in the critical range  $0 \leq \gamma \leq 0.5$ . To achieve acceptable lubricating conditions in this cam section the cam profiles should be designed for a HEC near the optimum value of 0.25 preferably for  $0.15 \leq \gamma \leq 0.25 \sim 0.30$ . It is further important that the range with  $\gamma$  near to 0.5 at the transition between cam nose and flank is passed as rapid as possible in order to shorten the periods with insufficient lubrication to the minimum possible extent.

### Ramp Heights

The ramps are provided to limit the impact during the valve opening and the seating velocity at the valve closing by the cam. To ensure that the opening and closing of the valves actually happens on the ramps, the ramp heights must exceed the values given below. The following ramp height requirements are equivalent ramp heights referred to the valve.

Ramp height for intake opening side,

$$h_R \geq C + \frac{F_0}{K_0} \geq 0.263 \quad (17.11)$$

For exhaust opening side,

$$h_R \geq C + \frac{F_0}{K_0} + \frac{F_G}{K_0} \geq 0.278 \quad (17.12)$$

Intake and exhaust closing side

$$h_R \geq C + \frac{F_0}{K_0} + \Delta h_R \geq 0.289 \text{ mm} \quad (17.13)$$

$\Delta h_R$  is the ramp height, required to compensate for valve cock action on the closing side.

### Ramp Rates

In general, the ramp rates in the constant velocity section of the ramp is assessed for a proper valve seating velocity  $V_r$  (mm/s) according to the relation

$$R_R = V_R/6N \quad (17.14)$$

Here,  $N$  = camshaft speed, rpm.

For a safe operation of valve train valve closing velocities in the range of 0.15–0.3 m/s are preferred.

### Cam Design Speed

For an assessed maximum camshaft speed  $N_{max}$  corresponding to the maximum engine overspeed, the cam design speed is given by,

$$N_c \geq \frac{N_{max}}{1.1} \quad (17.15)$$

For an assessed total cam length, the length of the positive acceleration pulse however also determines the length of the deceleration period and with that also the magnitudes of the deceleration whereby the later increases with decreasing length of the deceleration period. Deceleration phase length along with the spring loads control the contact stress values at the interface between cam and tappet, this becomes especially critical in the nose region of the cam where the radius of curvature is small and generally results in maximum contact stresses. Reduction of contact stresses can be achieved by an increase of the base circle diameter and to a certain degree by wider cams, whereby, however design limitations have to be taken into consideration for both dimensions.

### Choice of Exponents, Optimization of the Cam Profile

The exponents of the valve lift curve  $p$ ,  $q$ ,  $r$ ,  $s$  as well as the coefficient  $C_4$  determines the shape of the valve lift curve and with that the shape of the acceleration curve between the points  $x = 0$  and  $x = 1$ . As per the foregoing sections the magnitude of deceleration effects the required spring force as well as the radii of the cam contour with that also the cam tappet contact stresses and the hydrodynamic evaluation coefficients. A further reduction of the contact stresses can be achieved by an increase of the base circle dia. and to a certain extent by wider cams.

Whereby however design limitations have to be taken into consideration for both dimensions.

Problems regarding the optimization of the HEC in general do not occur with short cams. Contrary to short cams, the design of long duration cams normally does not involve any problems regarding the cam tappet contact stresses. Measures for the optimization of HEC are reduction of the base circle dia. an increase of the valve lift and a shorter cam length as a compromise regarding the gas exchange process. The optimization of the deceleration curve is finally accomplished by the proper choice of  $C_4$ .

**Hertzian Stress Calculation**

Maximum compressive stress at the contact between cam and follower is calculated by

$$\sigma_{max} = 0.564 \sqrt{\left[ \frac{P \left( \frac{\rho_1 + \rho_2}{\rho_1 \rho_2} \right)}{\frac{1-\mu_1^2}{E_1} + \frac{1-\mu_2^2}{E_2}} \right]} \tag{17.16a}$$

where,

$P''$	=	The normal load per unit width of the contacting members, N/mm
$\rho_1$	=	Radii of curvature of the cam, mm
$\rho_2$	=	Radii of curvature of the follower, mm
$\mu_1$	=	Poisson's ratio of cam = 0.3
$\mu_2$	=	Poisson's ratio of follower = 0.3
$E_1$	=	Modulus of elasticity of the cam, $N/mm^2 = 2.2 \times 10^5$
$E_2$	=	Modulus of elasticity of the follower, $N/mm^2 = 1.2 \times 10^5$

$$P' = \frac{P_{total}}{b \cos \alpha} \tag{17.16b}$$

Here,  $P_{total}$  = Inertia Force + spring force + Gaseous force

$b$  = Cam width, mm

In the valve cam design, Hertz's pressures up to 1500  $N/mm^2$  are proven, and calculated values showed sufficient safety margin with the proposed design.

In addition, the bearing stresses occurring on the contact surfaces of the cam and follower are determined for flat followers by using the formula i.e.,

$$\sigma_{bearing} = 0.418 \sqrt{\frac{P_{total} E}{b \rho_1}} \tag{17.17}$$

## 17.6 Valve Spring Calculations

### 17.6.1 Valve Spring Design

The deceleration in the valve train is ordinarily limited by the available valve spring force. Design loads of the valve spring must be high enough to ensure that the valve gear will remain in contact with the cam lobe at the highest anticipated speed. Lesser spring loads may result in a no follow or toss conditions, wherein the momentum of the valve gear exceeds the spring force so that the normal lift curve is not followed. For a safety factor the design loads of the spring should exceed those required to produce the necessary decelerations by a minimum of 30%. In order to minimize the surge, it is desirable to design the spring so that the natural frequency will exceed any resonance harmonic of appreciable amplitude, at maximum speed.

Experience has shown that the maximum surge should be limited to 2% of the valve lift. Thus, if the eleventh harmonic is the highest to have an amplitude of 2% the spring frequency should be twelve times maximum camshaft speed. Thus, for the minimum surge the wire should be the smallest diameter permissible within the design load limitations, and there should be a large no. of coils at a maximum pitch diameter.

In today's high-speed engines acceptable spring performance is normally obtained when the natural frequency is greater than the eleventh harmonic of camshaft rotational speed. For valve springs operating at less than the ninth harmonic of the camshaft rotational speed some type of frictional damper is advisable. The valve is supported at one end on cylinder head and at the other end on spring retainer cap in the groove in valve stem. It is shown in following Fig. 17.9.

Various means of avoiding valve spring surge are given in following Fig. 17.10 surge.

#### Design Criteria

The evaluation of the valve spring design is based on the following design criteria

- (1) The spring force must suffice to keep valve train parts in contact and to allow for friction and valve train vibrations.
- (2) The valve spring natural frequency must be sufficiently high in order to avoid excessive valve spring vibrations

The recommended ratios of the natural frequency of the valve spring,  $F_s$  to the rated camshaft speed,  $N_r$  are as follows:

*Linear spring with damper coils,*

$$\frac{f_s}{N_R} > 11 \quad (17.18)$$

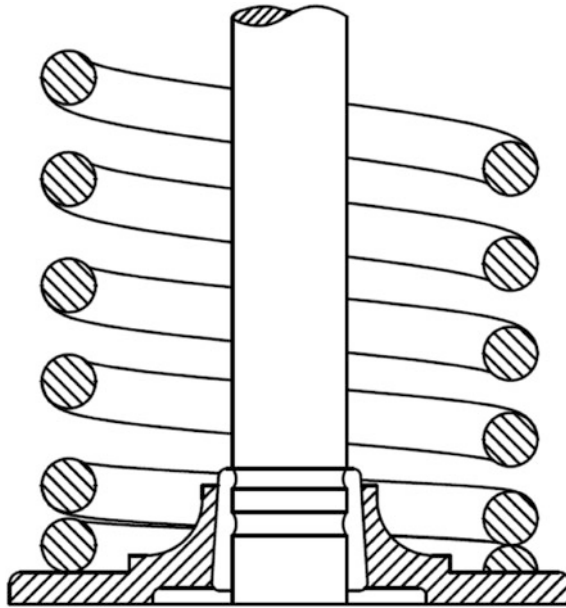


Fig. 17.9 Spring retainer cap

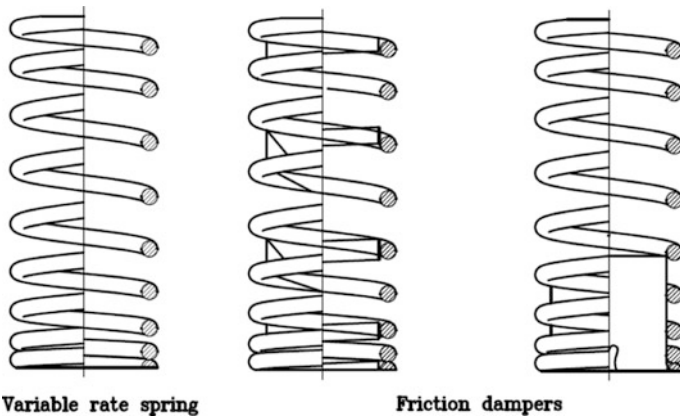


Fig. 17.10 Various means of avoiding valve spring surge



*Linear spring with damper coils*

$$\frac{f_s}{N_r} > 9 \quad (17.19)$$

(3) Valve spring stresses must be kept below permissible values.

*Natural oscillations of the spring*

$$n_N = 2.17 \times 10^7 \frac{d}{i_d D^2} \quad (17.20)$$

In dynamic respect the valve spring force must be sufficient to keep the valve train components in contact over the entire engine speed range including an allowance for friction and valve train vibrations

$$\frac{F_s}{F_d} \geq 1.1 \sim 1.2 \quad (17.21)$$

As per the experience with high speed engines this condition is met as far as valve spring forces exceed the theoretical deceleration force at maximum engine speed by at least 10–20% over the whole deceleration period.

The theoretical deceleration force at maximum engine over speed is obtained from the relation

$$F_d = 36N_{max}^2 (m_1 y_0'' + m_2 z_0'' / i) \quad (17.22)$$

(Its values are given at corresponding cam angle degrees in the form of graph.)

Here,

$N_{max}$  camshaft rpm at maximum engine speed  
 $m_1, m_2$  valve end and cam end mass respectively  
 $I$  instantaneous rocker ratio

Valve train natural frequency

It is obtained from the following formula,

$$f_N = \frac{30}{\pi} \sqrt{\frac{1000k_0}{m_1}} \quad (17.23)$$

Here

$f_N$  natural frequency, cycles/min  
 $k_0$  valve train stiffness, N/mm  
 $m_1$  valve end effective mass, kg

### Valve Train Stiffness

The valve train stiffness is determined by the ratio obtained by dividing a known force applied to the rocker arm valve end by the total deflection occurring at the rocker arm valve end due to this force.

$$K_0 = \frac{F}{d} \quad (17.24)$$

Preferably the valve train stiffness should be measured on the actual engine. If this is not possible a cursory evaluation of the deflections of the individual valve train components may be performed with the formulas given. Deflection of the rocker arm is calculated from the FEM model. Deflection of the pushrod,

$$d_p = \frac{Fl}{EA} i^2 \quad (17.25)$$

Here,

$l$ ,  $A$  = length and cross section area of push rod respectively.

Deflection of the camshaft,

$$d_c = \frac{Fa^2b^2}{3EJ} i^2 \quad (17.26)$$

Here,

$l$  span between camshaft bearing centres

$a$ ,  $b$  distance between cam centres and adjacent bearing centres.

$J$  flexural moment of inertia of camshaft cross section

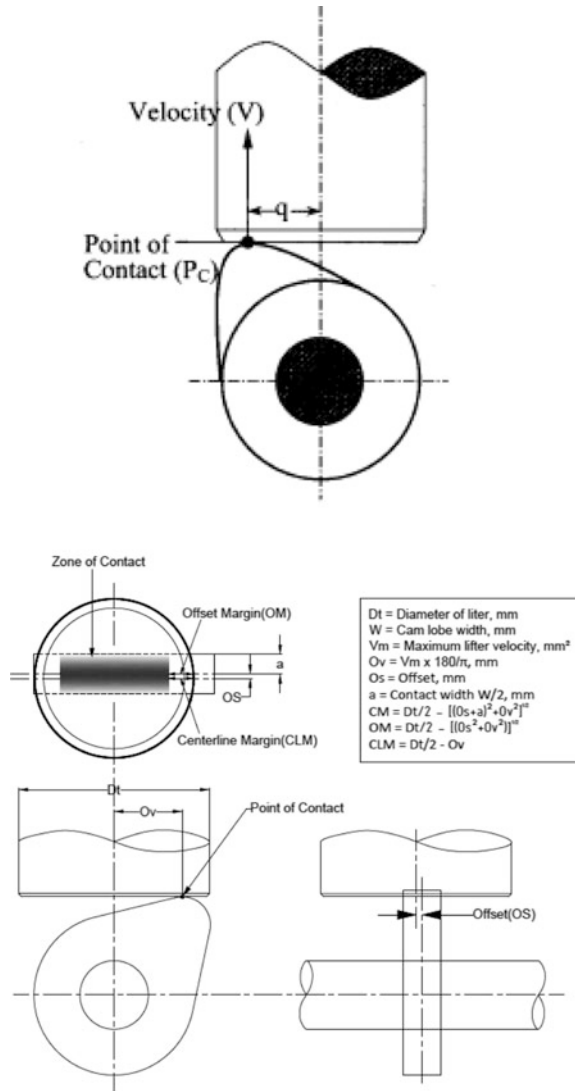
### Eccentricity of Contact

The cam to tappet contact varies with valve velocity and (1) the maximum eccentricity of contact along with cam width and (2) cam offset provided for uniform wear of the follower decide the required tappet diameter, Fig. 17.11. The eccentricity of contact is directly proportional to the cam velocity and it must be critically checked during design stage.

### Valve Train Simulation Using Simulation Tool

For kinematic analysis of valve train of an engine, AVL Excite TD simulation tool can be used which is solely meant for valve train analysis ([AVL Excite TD user manual](#)). Data in the form of mass and stiffness is given to the software. Cam design is carried out using the special module. Displacement, velocity, acceleration and forces against cam angle degrees are obtained as result. These results are validated against classical approach.

**Fig. 17.11** Eccentricity of contact with cam position (top); eccentricity provided by design for rotation and uniform wear of the follower (bottom)



### 17.7 1D-simulation—Valve Train Dynamics

Figure 17.12 shows *1D simulation* model overhead valve train. The valve train components consist of cam, tappet, push rod, rocker arm, and valves etc. The detailed description of each element and stiffness calculations are given below. The stiffness data of the element is calculated by using empirical relations, and finite element technique.

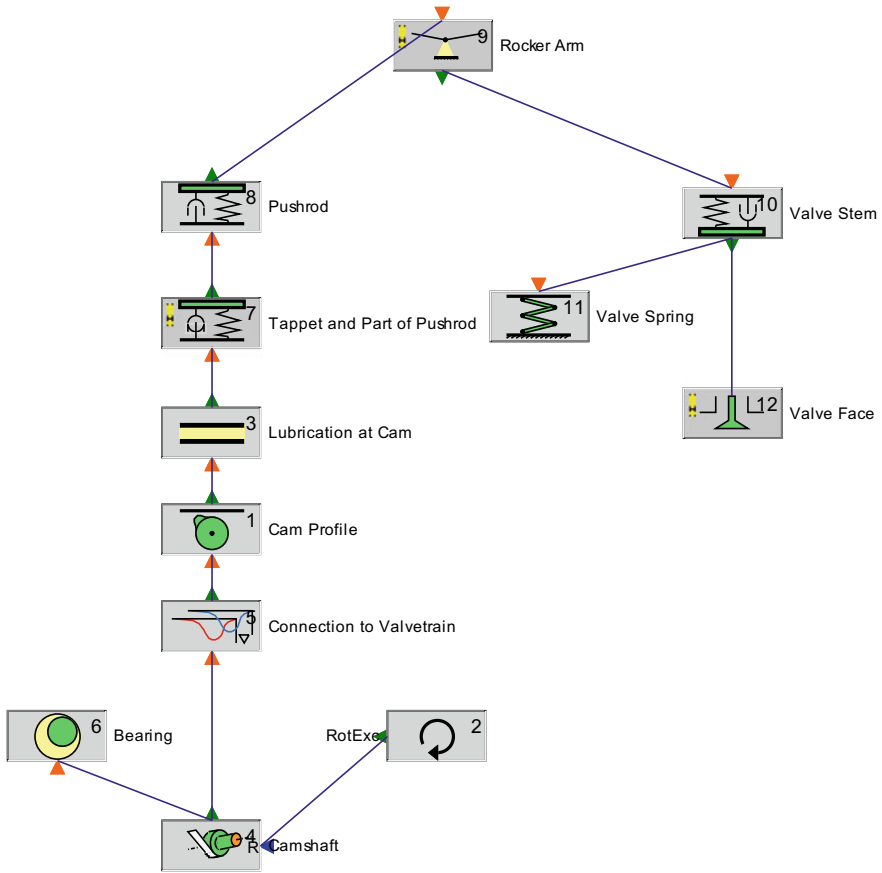


Fig. 17.12 Tycon model

**Cam Contour**

The cam profile was designed using *Cam Design* part of *Excite TD* and the analysis is carried out using *ISAC* method.

**Tappet and Portion of the Push Rod**

Spring/Damper/Mass element (*SDME*) is used to describe the properties of the tappet element. This element contains about one third the mass of the push rod and a portion of its stiffness. In the simulation assumed as, loss of contact is possible between the tappet and cam element.

**Element 2: Tappet and One Third Part of the Push Rod**

One spring/damper/mass element (*SDME*) is used to describe the properties of the tappet element. This element contains about one third the mass of the push rod and a portion of its stiffness. Loss of contact is possible between the roller tappet and the cam profile element.

**Stiffness Calculations for Tappet**

$$Stiffness = A \times E/L$$

$$stiffness = \frac{AE}{L} \tag{17.27}$$

where,  $A$ , cross sectional area =  $\frac{\pi}{4}(D^2 - d^2)$ , where  $D$  = Outer Diameter and  $d$  = Inner Diameter,  $E$  = Young’s Modulus  $L$  = Axial Length

The mass data is obtained from three-dimensional CAD model. In case of a roller tappet the stiffness is used from FEA model.

**Element 3: Pushrod**

Another SDME element is used to model the remaining part of the pushrod; there is no loss of contact possible between this and previous SDME element. The mass data is obtained from PROE model and stiffness is calculated analytically.

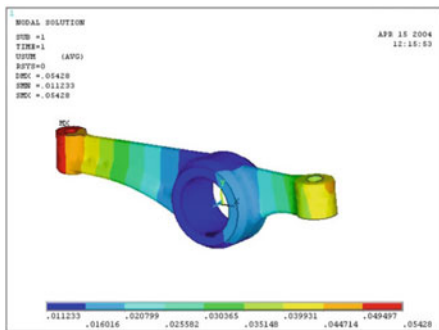
**Stiffness Calculations**

$$stiffness = \frac{AE}{L} \tag{17.28}$$

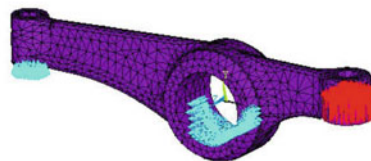
where,  $A$ , cross sectional area =  $\frac{\pi}{4}(D^2 - d^2)$ , where  $D$  = Outer Diameter and  $d$  = Inner Diameter  $E$  = Young’s Modulus  $L$  = Axial Length

**Element 4: Rocker Arm**

The rocker arm is modelled using a ROAR element. The mass is obtained using 3D CAD model. The stiffness is calculated using FEM model. For calculating the stiffness, the pushrod side portion of the camshaft is considered. The constraints are given as shown in the Fig. 17.13. A load of 100 N is applied at one end of the rocker arm. The arm behaves as a cantilever beam with a point load at the end. The



Displacement results



Boundary conditions

**Fig. 17.13** Results from FEM tool

deflection of the nodes on which load is applied is considered for stiffness calculations.

### Stiffness Calculations

$$\text{stiffness} = \frac{\text{Load}}{\text{Deflection}}$$

Displacement results by using Finite Element Analysis tool. The loss of contact is enabled between pushrod and rocker arm.

#### Element 5: Valve Stem

The valve is divided into two parts. The first part (Valve Stem) contains the stiffness and material damping of about half the valve and the mass of half the valve, all parts connecting the valve stem with the valve spring and the mass of the valve-side non-active coils of the spring. This part is represented in the TYCON model by another SDME element. Possible loss of contact between rocker arm and valve stem is considered in the model. At this element, the valve lash can be defined alternatively to its definition with the rocker arm data.

#### Element 6: Valve Face

The valve face is modelled as a VAFA element. Valve face is further divided into two parts. The first part is cylindrical, and the stiffness is calculated as usual. The second part is the bottom plate part, whose stiffness is calculated using the formula as given below. The mass data is obtained from CAD model. The stiffness of this part is calculated by considering the mean diameter of the remaining part of the valve.

### 17.7.1 Stiffness Calculations

$$\text{stiffness} = \frac{AE}{L} \quad (17.29)$$

where,  $A = \text{Cross sectional Area} = \frac{\pi}{4}D^2$ ,  $D = \text{Diameter}$ ,  $E = \text{Young's Modulus}$   
 $L = \text{Axial Length}$

#### First Cylindrical Part

$$\text{stiffness} = \frac{AE}{L} \quad (17.30)$$

$$A = \text{Cross sectional Area} = \frac{\pi}{4}d^2$$

- $d$  Diameter of valve stem
- $E$  Young's Modulus
- $L$  Axial Length

**Second Part (Bottom Plate Part)**

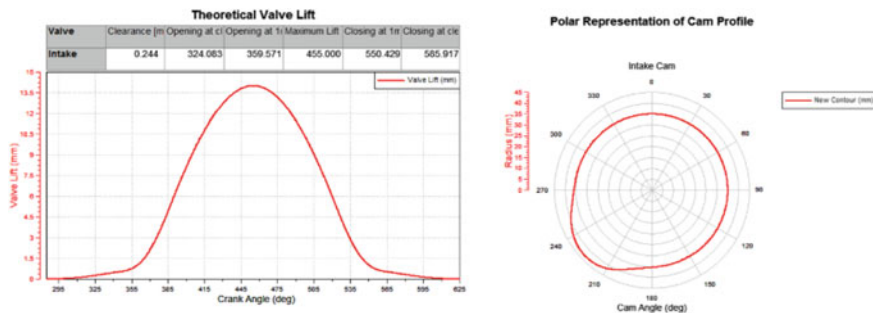
$$Stiffness = \frac{\pi E h^3}{0.628 R^2 \left( 2.54 - \left[ \frac{b}{R} \right]^2 \left[ 1.52 - \ln \frac{b}{R} \right] \right)} \tag{17.31}$$

- h* Height (thickness) of the plate part (4.8)
- R* Radius of the plate
- b* Load radius (valve stem radius)

**17.7.2 Results**

Typical results for a pushrod type valve train with roller tappet are summarized below. Figure 17.14 shows the theoretical valve lift and polar representation of the cam profile. The polar representation shows a large nose radius and a negative radius of curvature on flank which is typical for a roller tappet cam. The negative radius on the flank should be large enough to clear the grinding wheel during manufacturing. Typical values for grinding wheel diameters range from 200 to 400 mm. If the manufacturing setup is unknown at the time of design it is safe to keep negative radius greater than 200 mm.

The Fig. 17.15 shows the typical contact stress pattern for intake and exhaust cams for roller tappet configuration. The left-hand side image shows the intake side contact stress pattern at rated and zero (hypothetical) speed. The contact stress values at nose are higher at lower speeds. This is due to the fact that at lower speeds spring loads are getting transferred almost completely to cam- tappet contact and the radius of curvature at nose is on lower side. At higher speeds the inertia loads at flanks (during positive acceleration phase) are predominant leading to higher contact stress at flank.



**Fig. 17.14** Theoretical valve lift and polar representation of cam

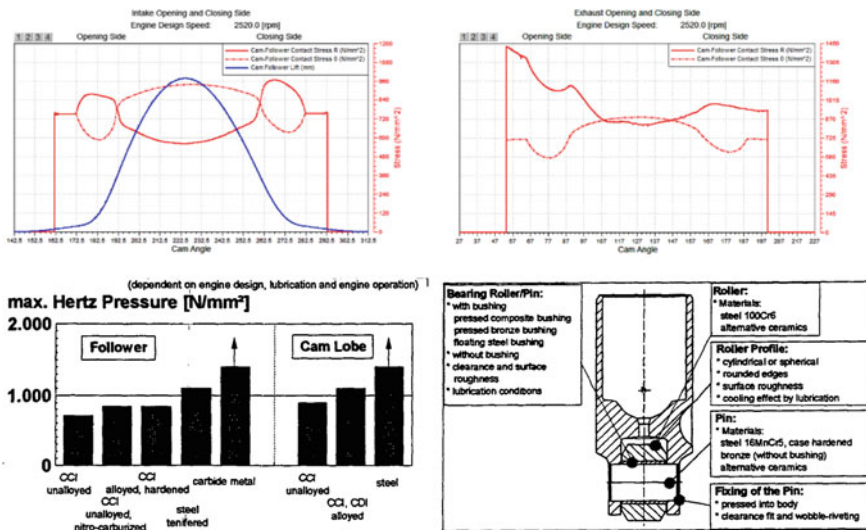


Fig. 17.15 Contact stress for intake and exhaust side

For exhaust, cam to tappet contact stresses are generally driven by the pressure inside the combustion chamber at the time of exhaust valve opening. This pressure (typically in the range of 5–15 bar) along with the spring loads are trying to close the valve resulting into high forces and subsequent contact stresses at the cam tappet interface.

Figure 17.15 also shows the typical contact stress (Max. Hertz pressure) limits for roller tappets and typical design features for roller tappet (Korte et al. 1997).

Figure 17.16 shows the valve acceleration profiles for intake and exhaust.  $A_f$  and  $A_n$  are the max acceleration values at flank and nose. It is recommended to keep the ratio of  $A_f/A_n$  less than 2.5. Intake cams generally have smaller durations and hence result in larger  $A_f/A_n$  values, which may result in jerk and need to be analysed

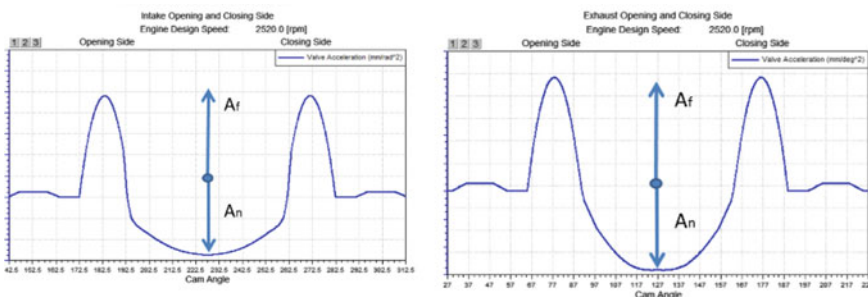


Fig. 17.16 Valve acceleration profile for intake and exhaust



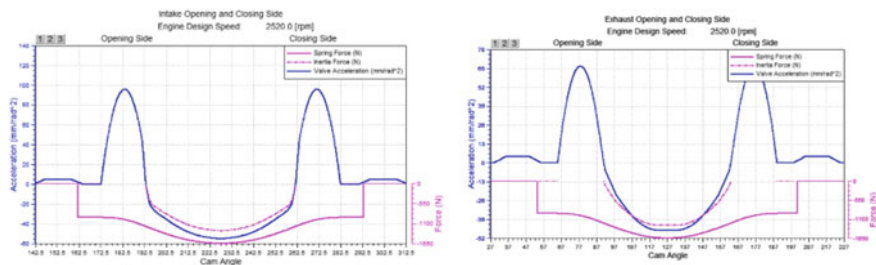


Fig. 17.17 Spring cover factors

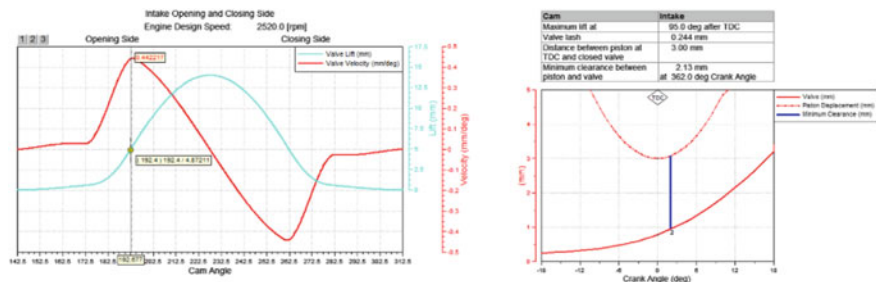


Fig. 17.18 Max velocity point and piston to valve distance

closely. Exhaust on the other hand do not suffer from this problem due to higher durations.

Figure 17.17 shows the spring cover factor. This is essential to keep the valve train parts in contact even during overspeed conditions. Typically, a cover factor of 1.2–1.3 is used at overspeed condition for safe operation of the valve train.

Figure 17.18 shows the lift values at max velocity point and valve to piston distance during operation. Max velocity point should generally occur at one third to half of total valve lift. This helps in reducing the sliding velocities at the rocker arm to valve tip interface. The target should be to keep the rocker arm perpendicular to valve tip at max valve velocity.

Figure 17.19 shows the typical valve bounce behaviour at valve closing event with change in operating speed. A threshold value is generally used depending on operating speeds and application. In the absence of any guidelines 1% of total valve lift can be used for valve bounce limit. The valve closing speeds go on increasing with change in speed and show exponential increase beyond a threshold operating speed. Continuous operation at above this speed should be avoided for safe operation of the valve train.

Figure 17.20 shows the pushrod force diagrams for intake and exhaust. For intake the max force values generally occur at the flank region while for exhaust the max force values occur at the time of opening due to cylinder pressure inside the combustion chamber. One more area of interest is the middle portion of the diagram

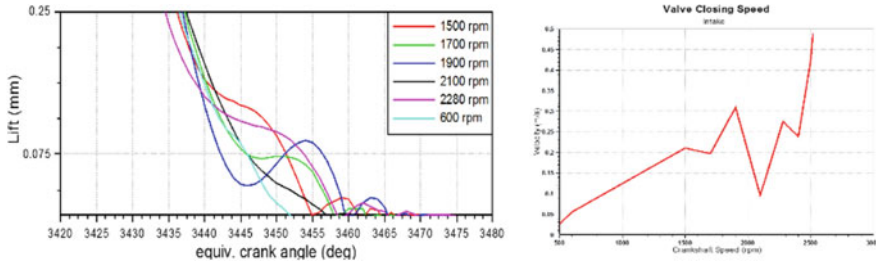


Fig. 17.19 Valve bounce and valve closing speeds

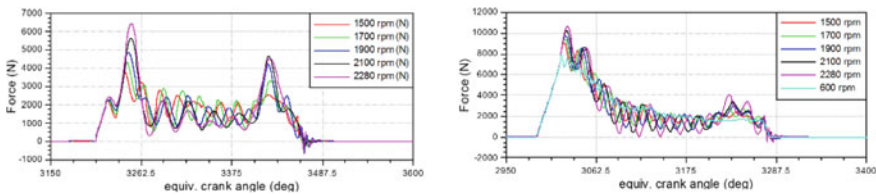


Fig. 17.20 Pushrod force for intake and exhaust

where the valve train oscillates at its natural frequency and variation can be seen in the pushrod force values. Design should aim to avoid pushrod force becoming zero during operating speed range as it can cause loss of contact and severe damage to the valve train. The max force values from above diagrams can also be used for buckling analysis of the pushrod.

**Tribological Considerations in the Design and Operation of Cams**

Whilst reliable and efficient use of non-conforming machine elements such as gears, rolling contact bearings and cams has long been recognized as an essential requirement in the operation of industrial machinery it is only in the last twenty years that better understanding of what goes on between the surfaces in contact has been permitted a gradual improvement in their design and performance. The lubrication factor incorporates lubricant selection related to the required bearing performance in terms of the elastohydrodynamic concept. A thorough analysis of the problems in cams is studied by Naylor in which the main wear mechanisms are defined (Naylor 1967). Elastohydrodynamic lubrication theory is described and is related to the mechanisms of pitting, scuffing and other concepts such as the flash temperature concept.

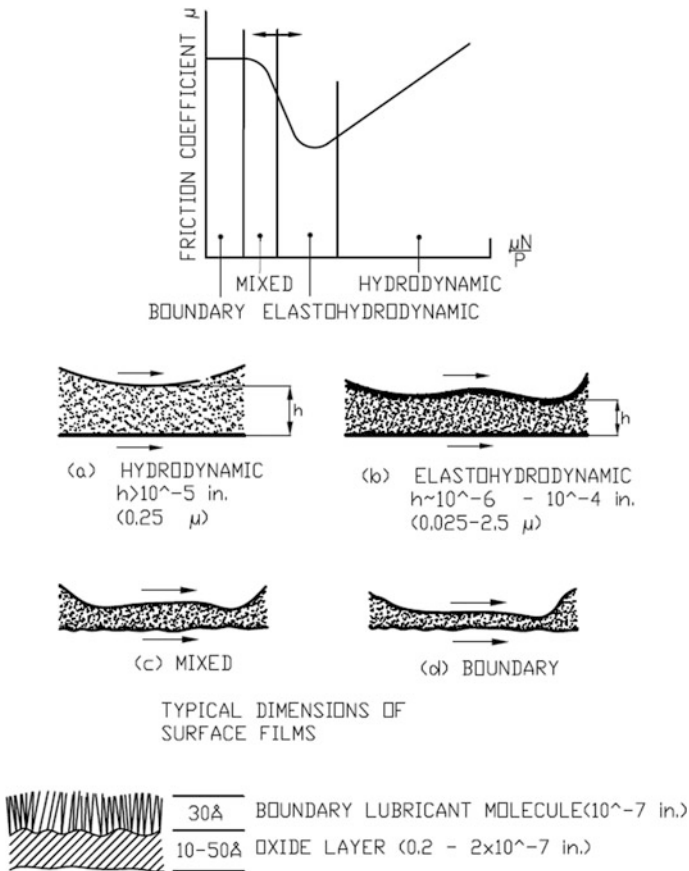
The dominant requirements in the operation of cams are to reduce the probability of premature surface failure. Study of the mechanism of elastohydrodynamic lubrication is essential if failure due to wear is to be explained. The equation of film thickness separating an equivalent cylinder in nominal line contact with a plane has been expressed as

$$1.95(\alpha\eta_0 u)^{\frac{8}{11}} \left(\frac{E'}{\omega}\right)^{\frac{1}{11}} R^{\frac{4}{11}} \tag{17.32}$$

For condition of point contact the for film-thickness developed by Archard and Cowking is expressed as (Archard and Cowking 1965), Fig. 17.21,

$$h_0 = 2.04 \left| 1 + \frac{2R_y}{3R_x} \right|^{-0.74} |\eta_0 x \mu|^{0.74} R^{0.407} \left| \frac{E'}{\omega'} \right|^{0.074} \tag{17.33}$$

An alternative form in non-dimensional terms has been given by Dowson  
For a cylinder near a plane,



**Fig. 17.21** Lubrication Regimes

$$H_{min} = \frac{2.65G^{0.54}U^{0.70}}{W^{0.13}} \tag{17.34}$$

And for a sphere near a plane,

$$H = \frac{1.4(GU)^{0.74}}{W^{0.074}} \tag{17.35}$$

If cams operate under condition of hydrodynamic or elasto-hydrodynamic lubrications these equations can be used to calculate the film thickness. From this the quality of the lubrication film in relation to the roughness of the surface is determined thus establishing the likely mode of lubrication e.g. hydrodynamic, mixed or boundary, Fig. 17.21.

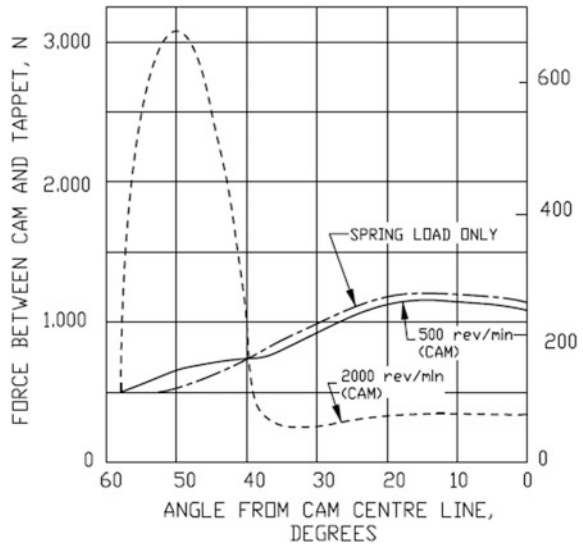
In the design of cam systems, it is usual to determine contact stress together with some considerations of the relative sliding velocity. It is therefore necessary to establish the load pattern and instantaneous radius of curvature with the cam angle. Figure 17.22 shows typical data for an automotive cam.

**Typical Automotive Cam System**

In practice surfaces are not perfectly smooth. In the case of cams for example a surface finish of 0.3 C.L.A. is fairly typical. The geometrical factor which governs the lubrication regime is defined as,

Film thickness ratio  $R$  (or  $A$ ) = calculated film thickness/summation of surface roughness

**Fig. 17.22** Variation in instantaneous radius of curvature and cam tappet force



where the surface roughness term is usually defined as

$$\sigma = \sqrt{\sigma_1^2 + \sigma_2^2} \tag{17.36}$$

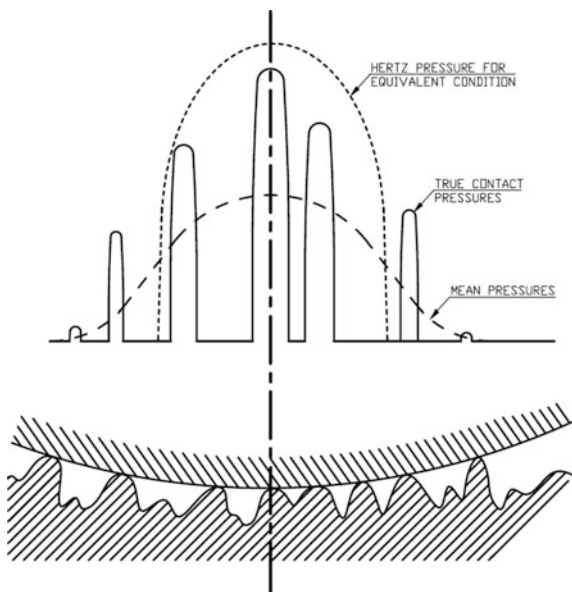
Here,  $\sigma_1$  and  $\sigma_2$  are the roughness of the two surfaces. Full Elastohydrodynamic lubrication conditions are expected to exist when  $R > 4$  and it is significant that the wear behaviour of non-conformal lubricated contacts has been shown to be related to this ratio. Figure 17.23 shows the basis for lubrication of rough surfaces. Dawson showed its importance in pitting experiments conducted on discs. Tallian et al. also related it to surface fatigue in nominal point contact operation. The results of their work together with others enabled the specification of the lubrication life factor in rolling element bearings.

In connection with the effect of surface roughness it is necessary to make mention of current research into microscopic elastohydrodynamic action. Archard discusses this aspect in relation to the results of other workers in which he analyses the plausibility of the Elastohydrodynamic lubrication theory being applied to the individual asperities.

As Archard states, it is necessary to recall that one of the simple requirements of the Elastohydrodynamic lubrication theory is that the results must be consistent with both the elastic equations and with Reynolds equation.

In addition to surface roughness considerations the determination of film thickness is affected by factors such as variation in the loading and the thermal behaviour in the contact zone.

**Fig. 17.23** Basis for lubrication of rough surfaces



### **Variation of Loading and Other Parameters**

The operation of cams introduces a squeeze action at the surfaces in contact. This arises as a result of the variation in e.g. load and relative radius of curvature with respect to time. The classical approach to the solution of elasto-hydrodynamic problems assumes steady state conditions and the extent to which the squeezing action modifies the behaviour have been investigated by Vichard.

It is seen that the squeeze components act effectively as a viscous damping phenomenon in which the variations of the external parameters such as load etc. are damped down.

### **Thermal Aspects**

The temperature which controls the film thickness is the surface temperature of the solids in the inlet region of the contact. For a wide range of load, speeds and lubricant properties the loss of load film due to thermal effects is strongly influenced by the rolling velocity and inlet velocity of the lubricant. Whilst it is insensitive to the change of load.

### **Failure Conditions**

From calculation of the film thickness and knowledge of the roughness parameters of the surface in contact the regime of lubrication can be specified. It is then possible to consider the probability of failure in relation to the particular type of cam follower operation and working environment. The basic types of failure in cam operations are well documented; they are pitting scuffing and polish wear.

Failure by scuffing and pitting affects all non-conforming machine elements and has been the subject of investigation for many years. Scuffing as a consequence of increased asperity contact, arises when relative sliding occurs in the absence of adequate fluid film lubrication. It is not primarily time dependent but it is likely to occur rapidly.

**Pitting** is dependent both on running time and contact stress. The fatigue due to high cyclical stress on the surface, initiates a crack over time and the propagates to produce pits.

**Polish wear** causes a smooth burnished appearance on the surface. It may be a transitional case between scuffing and pitting, assisted by chemical action involving the oil.

As scuffing occurs when there is an increase in asperity contact the system is operating in the boundary or mixed lubrication regime. Under conditions where the speed, load and bulk temperature of the surfaces are sufficiently low reducing the surface roughness may lessen the tendency to scuff.

The thermal concept in relation to the scuffing wear is not new. In 1937 Bloc presented his idea of a critical contact temperature which has since become known as the flash temperature theory. The hypothesis is that the surface will scuff if the total contact temperature exceeds a critical level. Bloc has reviewed experimental results reported in the literature in which there are indications that the total contact temperature just prior to scuffing is not constant. Depending on the conditions any one of the three criteria, total contact temperature, film thickness, and friction power intensity remains approximately constant within specific speed range conditions.

## Pitting

The method developed for relating the film thickness ratio to fatigue life in rolling elements is based on many years of careful investigation. Full Elastohydrodynamic lubrication conditions are implied when  $R > 4$ , but improve resistance to fatigue is evident when  $R > 1.2$ . Thus, the extent and nature of the asperity contact is one aspect which affects fatigue life. Early theories on rolling bearing fatigue life assumed that it was directly related to subsurface stress conditions. Under these conditions the failure is initiated at a depth below the contact area where the shear stress is a maximum. Sub surface stresses are being analysed by use of optical methods using a synthetic sapphire insert in one of the discs. It is hoped that finding will be relevant to the situation that exists between a cam and non-rotating follower.

More recently the rolling four ball geometry has been used to investigate rolling contact fatigue behaviour of different lubricants. Calculation can be made to establish the film thickness with respect to the cam angle and nominal operating conditions based on ideal smooth surfaces operating under isothermal conditions. By relating to the surface roughness, the quality of the film can be assessed and related to in a semi quantitative manner to possible failure mechanisms.

## Experimentation

### Experimentation Methods Used in the IC Engine

IC engine valve trains are often limited to the measurement of valve displacement and strain in rocker arms or other valve train components. Non-contacting proximity probes can be used to measure displacement in a running engine which is an advantage, but their small range limits to investigation of motion at the opening or closing of a valve.

Kreuter et al. measured forces, valve acceleration, and EHD oil film thickness in motored engine and observed that forces and accelerations are the most important criteria to evaluate valve train dynamic performance (Kreuter and Maas 1987). While experimental measurements of displacement and velocity are useful, studies done on the non-automotive cam follower systems have shown the advantages of acceleration measurements for dynamic analysis.

There are two fundamental reasons for this. Accelerometers typically have larger bandwidth than velocity transducers, displacement transducers or strain gauges and higher derivatives of a function tend to exaggerate the system's dynamic behaviour. Seidlitz found that a valve train can be modelled as a linear spring despite the presence of some of the nonlinearities (Seidlitz 1989).

Valve motion measurements under dynamic conditions might be made by using either optical tracking or a linear variable differentia transformer. However, both these approaches are intrusive in that the engine is modified to the point that it cannot be run normally

An extremely simple and rugged transducer the proximity probe provided the basis for this measurement system. The proximity probe used in this application has a linear range of 1.0 mm, so both the beginning and ending of the valve event are accurately reproduced. However, this transducer does not provide useful information on valve for periods of the valve event when the lift exceeds 1.0 mm.

Calibrations at elevated temperatures were carried out by bathing the probes in heated engine oil. Crank angle information was obtained by attaching an encoder to the engine crankshaft. This encoder provided cycle and crank angle pulses use to start and drive the synchronous high-speed scanning of the two proximity probe signals.

### Experimental Setup for the Valve Lift Measurement

#### Experimental Setup

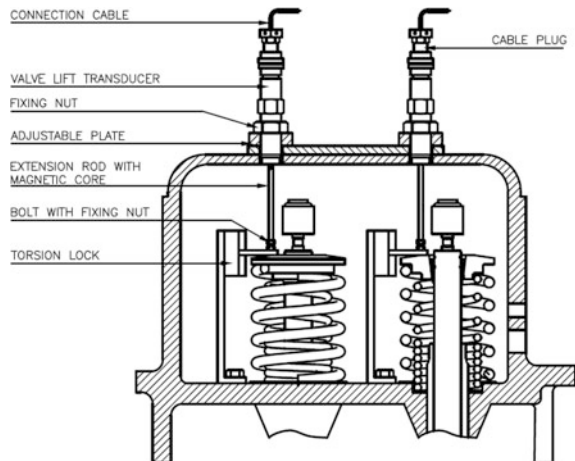
Experimental setup for valve lift measurement is as shown in the above figure. Here modifications are made in the rocker cover. A Linear Variable Differential Transformer (LVDT) is used. It is inserted through the rocker cover. Height of LVDT is adjusted with the help of adjustment plate. A fixing nut arrangement is also there. Needle of LVDT rests on the spring retainer cup. A slight groove is made in spring retainer cup to accommodate needle of LVDT. Figure 17.24 shows the experimental setup.

A torsion lock arrangement is made to avoid rotation of the valve as valve is rotating during actual running of the engine. Torsion lock is in form of a plate which is bent in the L shape. A groove is made in it. It is fixed to the cylinder head. A thin rod is brazed to the spring retainer cup and it is made to pass through the groove in the plate. As the valve lift and rotates t rod slides in the groove in the L plate. Thus, rotary motion of valve is converted into the translational motion. Connection of LVDT is given to data acquisition system. It gives results for the valve lift, which on differentiation gives the velocity and acceleration.

#### Other Experimentation Methods

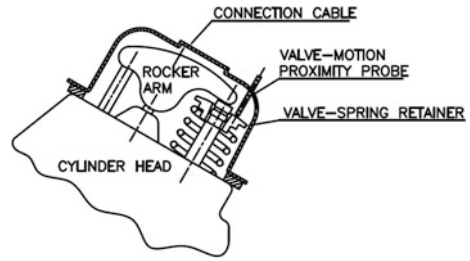
The experimental setup is shown in the above Fig. 17.25. Here a proximity probe is attached over the spring retainer cap, which is having a range of 1.0 mm only. So, it can reproduce data while opening and closing of the valve. But it cannot be used for wider ranges of the valve motions. This experimentation is performed by Herrin (1982).

**Fig. 17.24** Valve lift measurement





**Fig. 17.25** Valve motion measurement



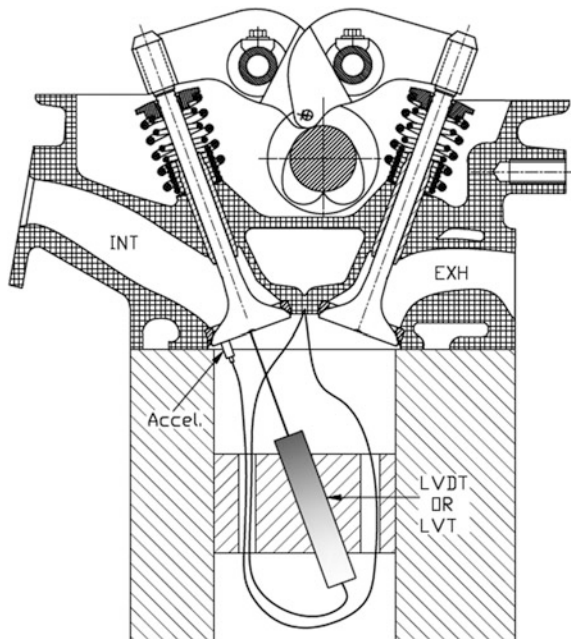
Experimental arrangement is as shown in the above Fig. 17.26 this is performed by Robert L. Norton for analysing the vibrations in IC engine valve train (Norton et al. 1998). He attached LVDT, LVT and accelerometer to the head of valve. This experimentation is performed for OHC engine.

Typical oscillograph traces for valve lift, velocity and acceleration are as shown in Fig. 17.27. Similar trends are obtained in the experimental results.

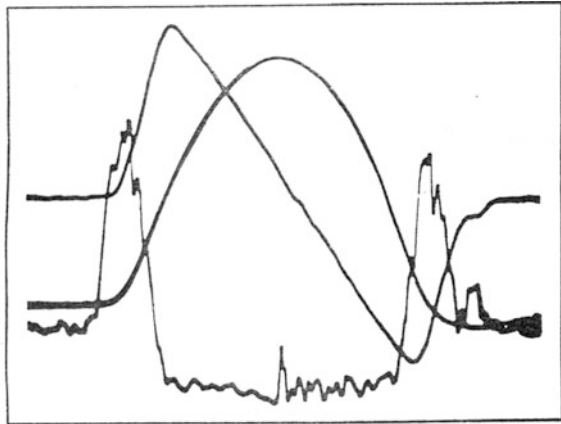
### Literature Survey

A model for valve train dynamics was presented by Philips et al. which aims at both accuracy and efficiency. The model results show good agreement with measured accelerations for a DOHC engine with direct acting bucket tappets. Moreover, the model allows one to quickly gain an insight into the dynamics of valve trains (Philips et al. 1989). A method for constructing a cam profile for high performance engines was developed by breaking the cam profile into ten separate polynomial

**Fig. 17.26** Measurement of vibrations



**Fig. 17.27** Oscillograph traces



events, defined by boundary conditions at both ends of the event (Park and David 1996). The separate events allowed the cam profile to meet several kinematics constraints and gave the profile fifteen degrees of freedom for optimization. The degree position of the camshaft was locally non-dimensionalised with respect to each event in order to simplify the solution of polynomial coefficients. In addition, the cam profile was made mathematically symmetric applying the coefficient solutions from the opening side to the closing side.

The profiles of finger followers resulting from steady, non-catastrophic wear processes have been computed by combining a simple wear law and an elasto-hydrodynamic/boundary lubrication transition model with a new kinematics analysis (Bell et al. 1985). The predicted profiles exhibit good qualitative agreement with experimental observations for two different designs. Wear appears to be influenced predominantly by the state of boundary lubrication and is greatest in possibilities where the velocity of the contact over the follower is small. A mechanism of variable valve actuation is called variable rocker arm (VRA). VRA has the capability to control both valve event and valve lift. VRA is compact and simple. It consists of mainly two components an output cam and rocker arm. This could produce less movement and less inertia than other mechanisms. This mechanism can be applied to various valve trains such as DOHC, SOHC, and push rod. The VRA has been tested with a 4-stroke single cylinder engine to measure the torque, fuel consumption and emissions. Besides controlling the valve event and valve lift, the VRA can also be operated with variable timing control if desired (Anontaphan 2003).

A multipurpose analysis tool developed which was aimed at addressing all design issues arising in various stages of valve train development (Keribar 2000). Its capabilities include polynomial cam design, valve train mechanism kinematics, quasi-dynamic analysis, spring design/selection, multibody elastic analysis of a single valve train with cam follower and bearing tribology, and multi valve train dynamics with camshaft torsional vibrations. This paper describes the methodology

and its capabilities in general and selected key sub models, specifically those for valve springs, hydraulic valve lash adjuster, cam follower tribology and bearing oil films in more detail. Comparisons of predictions to experimental data are also presented as well as examples of applications. Giles reviewed some of the fundamentals of valve train engineering as predicted by the engine designer (Giles 1966). Valve proportions are considered in terms of the engine volumetric efficiency, valve operating temperature and stress conditions. Other factors influencing valve durability such as valve train dynamics, cylinder head and seat design and material selection etc. are also discussed. Common types of valve failures and their design and their causes are appraised as a means of.

To fulfil the increasing requirements modern heavy-duty diesel engines are using valve train configurations with roller followers, designed as roller tappets or roller levers. While these roller followers are well known engine components there is a great demand for the enhancement of functional properties and simultaneous cost reduction. Main areas for the design work are the base design of body or lever with roller chamber, push rod area and lever geometry and especially the roller bearing together with the assembling technology (Korte et al. 2000). The simple measurement system was developed to quantify compliance in an engine valve train and to pinpoint accurately valve opening and closing under dynamic operation (Herrin 1982). The measurement was used to quantify total valve train compliance at the time of valve opening and closing for broad ranges of engine speed and oil temperature. This information allows valve timing to be predicted accurately for use in both engine thermodynamic cycle analysis and cam design.

For valve trains that operate with roller followers at relatively high contact stress assembled camshafts are a cost-effective solution as compared to camshafts machined from forged bar stock. Forged bearing steels and to a lesser extent powder forged steels, have been the materials of choice for the manufacture of cam lobes for assembled camshafts. Sintered alloys offer an attractive alternative to forged steel because very accurate cam lobes can be manufactured via pressing and sintering. However, the use of sintered alloys has been limited by their relatively low rolling contact fatigue properties (Blanchard et al. 2000). The vibration characteristics of a valve train were analysed over a range of operating speeds to investigate and demonstrate the advantages and limitations of various dynamic measurements such as displacement, velocity and acceleration (Norton et al. 1998). The valve train was tested in a motoring fixture at speeds of 500–3500 camshaft rpm. The advantages of analysing both time and frequency domain measurements are described.

One of the most severe problems in the valve train operation is the wear of the valve face or seat. The dynamic study of the valve mechanisms can be applied to this problem. It can be concluded that the impulse force acting on the valve at the closing moment is the most effective factor to influence this problem. This paper describes the use of five mass models to simulate the valve mechanisms dynamically. The results of the calculation agree well with the experimental data and the new knowledge acquired indicates that the impulse force does not necessarily increase with the rising cam speed (Daniel Clark Park and David 1996).

## References

- Anontaphan T (2003) A study of mechanical continuous variable rocker arm. SAE Paper, 2003-01-0022
- Archard JF, Cowking EW (1965) Elastohydrodynamic lubrication at point contacts. Proc Inst Mech Eng Conf 180(2):47–56
- Bell JC, Davies PJ, Fu WB (1985) Prediction of automotive valve train wear patterns with simple mathematical models. In: Proceedings of the 12th Leeds–Lyon symposium on tribology: mechanisms and surface-distress, Paper XI iii, pp 323–333
- Blanchard P, Nigarura S, Trasorras JRL, Wordsworth R (2000) Assembled camshaft with sintered cam lobes: torsional fatigue strength and wear performance. SAE Paper 2000-01-0397, pp 1–3
- Giles WS (1966) Fundamentals of valve design and material selection. SAE Paper, 660471, pp 1–20
- Herrin RJ (1982) Measurement of engine valve train compliance under dynamic conditions. SAE Paper 820689, pp. 2645–2653
- Herrin RJ (1982) Measurement of engine valve train compliance under dynamic conditions. SAE Paper, 820768, pp 1–3
- Keribar R (2000) A valve train design analysis tool with multiple functionality. SAE Paper, 2000-01-0562, pp 1–3
- Korte V, Barth R, Kirschner R, Schulze J (1997) Camshaft/follower-design for different stress behaviour in heavy duty diesel engines: SAE Paper 972776
- Korte V, Glas T, Lettmann M, Krepulat W, Steinmetz C (2000) Cam roller follower design for heavy duty diesel engines. SAE Paper, 2000-01-0525, pp 1–2
- Kreuter P, Maas G (1987) Influence of hydraulic valve lash adjusters on the dynamic behavior of valve trains. SAE technical Paper 870086
- Naylor H (1967) Cams and friction drives. Proc Inst Mech Eng Conf 182(1): 237–261
- Norton RL, Stene RL, Westbrook J, Eovaldi D (1998) Analyzing vibrations in an IC engine valve train. SAE Paper, 980570, pp 1–3
- Park DC, David JW (1996) Development of a locally nondimensional mathematically symmetric cam profile for optimal camshaft design. SAE Paper, 960355
- Philips PJ, Schamel AR, Meyer J (1989) An efficient model for valve train and spring dynamics. SAE Paper, 890619
- Seidlitz S (1989) Valve train dynamics-a computer study. SAE technical Paper 890620
- AVL TYCON user manual
- Wang Y (2006) Introduction to engine valve train